




Cite this: *Mater. Adv.*, 2023,  
4, 6353

# The particle size control of ruthenium-encapsulated hollow silica sphere catalysts for the hydrogenation of carbon dioxide into formic acid

Tetsuo Umegaki, \* Eiji Nagakubo, Kenjiro Saeki and Yoshiyuki Kojima

In the present study, the control of particle size of ruthenium-encapsulated hollow silica catalysts is reported. For controlling the size, the preparation conditions of carbon sphere template particles for fabricating hollow silica sphere support materials were investigated. The particle size of templates depends on the settling temperature of glucose solutions before hydrothermal treatment for template preparation and glucose concentrations. Especially, the particle size of hollow spheres decreases with a decrease in glucose concentrations. The results of Fourier transform infrared-attenuated total reflectance (FTIR-ATR) spectroscopy indicated that the hydrolysis reaction of glucose proceeded at high settling temperatures before hydrothermal treatment and in solutions with high glucose concentrations to give carbon sphere templates, and templates with small particle size were obtained following the hydrothermal treatment. Ruthenium-encapsulated hollow silica sphere catalysts prepared using hollow silica sphere supports with small particle size contained highly dispersed active ruthenium species and exhibited high catalytic activity for the hydrogenation of carbon dioxide into formic acid.

Received 27th June 2023,  
Accepted 27th October 2023

DOI: 10.1039/d3ma00331k

rsc.li/materials-advances

## 1. Introduction

Oxygen-containing compounds, such as carbon dioxide and water, are stable in the oxidative atmosphere of the earth. Especially, the emission of massive amounts of carbon dioxide due to human activities and the accumulation of carbon dioxide has gradually increased in the atmosphere, which are unmanageable by natural processes, such as photosynthesis for recycling carbon dioxide, resulting in various severe climate changes by its greenhouse effect. Chemical reactions of carbon dioxide with various reductants, such as hydrogenation reactions, have been regarded as one of the promising processes for the effective use of oxygen-containing compounds.<sup>1–6</sup> The hydrogenation of carbon dioxide and inorganic carbonates (alkali carbonates, ammonium carbonate, and so on) to form formic acid has attracted much attention as an energetically effective process, and various effective catalysts for the reactions have been reported.<sup>7–17</sup> Our research group has investigated metallic ruthenium particle catalysts prepared by an originally developed liquid-phase reduction process from a ruthenium salt.<sup>10</sup> The ruthenium particle catalyst exhibited high activity for the hydrogenation of supercritical carbon dioxide into formic acid in a methyl alcohol-based solution. The catalytic activity increased

with the addition of an appropriate amount of water; however, excess amounts of water caused a drastic decrease in the activity because of the dissolution of active metallic ruthenium species.

In the present study, we investigated the encapsulation effect of hollow silica sphere supports to improve the activity of the metallic ruthenium particle catalyst for the hydrogenation of supercritical carbon dioxide into formic acid. Hollow sphere particles have the advantages of easily controllable shell thickness at the nano size, effective immersion of active species into the inner pores of the shell, and high dispersion of active species in the shell.<sup>15,18–27</sup> Their dispersion allows the control of the morphology of hollow spheres, including pore structures. The encapsulated catalysts with precisely controlled morphologies exhibited high catalytic performances.<sup>15,21,24–27</sup> We investigated the effect of particle size control of hollow silica sphere supports on the activity of ruthenium-encapsulated hollow silica sphere catalysts for the hydrogenation of carbon dioxide into formic acid. In the present study, we also provide new insights into the control of the size of spherical carbon particle templates prepared from glucose for preparing hollow silica sphere supports.

## 2. Experimental

### 2.1. Catalyst preparation

Ruthenium-encapsulated hollow silica spheres were prepared using a spherical carbon particle template according to the

Department of Materials and Applied Chemistry, College of Science and Technology,  
Nihon University, 1-8-14, Kanda Surugadai, Chiyoda-ku, Tokyo, 101-8308, Japan.  
E-mail: umegaki.tetsuo@nihon-u.ac.jp



previous studies.<sup>28–31</sup> For the preparation of template particles, glucose (16.05–42.80 g, FUJIFILM Wako Chem. Co.,  $\geq 98.0\%$ ) was dissolved in deionized water (100 mL) with ethyl alcohol (3 mL, FUJIFILM Wako Chem. Co.,  $\geq 99.5\%$ ) in a Teflon-lined stainless autoclave. After stirring at 298 K for 30 min, the solution was kept at settling temperatures in the range of 323–373 K for 1 h without stirring, and then, hydrothermally treated at 443 K for 9 h. The resulting suspension was filtrated and dried at 373 K for 2 h to obtain the template particles. Using the obtained templates, hollow silica spheres were prepared by a sol-gel based method. The templates (0.2000 g) were mixed with cetyltrimethylammonium bromide (CTAB, 0.0930 g, Kanto Chem. Co. Ltd,  $\geq 96.0\%$ ) and L(+)-arginine (0.0871 g, FUJIFILM Wako Chem. Co.,  $\geq 98.0\%$ ) in a mixed solution of methyl alcohol (15 mL) and deionized water (2 mL). After stirring the solution at 333 K for 30 min, tetraethoxysilane (TEOS, 0.56 mL, FUJIFILM Wako Chem. Co.,  $\geq 98.0\%$ ) was added into the solution, and then, the solution was stirred at 333 K for 2 h. After centrifuging (6000 rpm, 5 min) and washing with ethyl alcohol for 3 times, the samples were dried in a dedicator, followed by calcination at 673 K for 3 h to obtain hollow silica spheres. Precursors of ruthenium-encapsulated hollow silica spheres were prepared by an impregnation method with a methyl alcohol solution (15 mL) of ruthenium chloride hydrate ( $\text{RuCl}_3 \cdot n\text{H}_2\text{O}$  ( $n \approx 1.87$ ), FUJIFILM Wako Chem. Co.,  $\geq 85.0\%$ ) using hollow silica spheres degassed at 423 K for 6 h under vacuum condition. After stirring at 298 K for 3 h, the suspension was solvothermally treated in a Teflon-lined stainless autoclave at 423 K for 10 h followed by centrifugation (8000 rpm, 10 min) and drying to obtain ruthenium-encapsulated hollow silica sphere catalysts.

## 2.2. Characterization

The morphology of host hollow silica spheres was analysed using a SM-300 scanning electron microscope (SEM, TOPCON) and a FE2000 field emission transmission electron microscope (FE-TEM, Hitachi). Particle size distributions of spherical carbon templates prepared under various preparation conditions were evaluated from the result of SEM measurements. The bonding state of glucose in aqueous solutions before and after the hydrothermal treatment at temperatures in the range 323–373 K was acquired using an IRSpirt spectrometer (Shimadzu Co. Ltd) with a diamond single-reflection attenuated total reflectance (FTIR-ATR) device. Duplicate spectra per sample were obtained with 400 scans per spectrum at a spectral resolution of  $4\text{ cm}^{-1}$  in the wavenumber range from 5000 to  $400\text{ cm}^{-1}$ . Powder X-ray diffraction (PXRD) patterns of the catalysts were recorded using a MultiFlex X-ray diffractometer (Rigaku) with Cu  $K_\alpha$  radiation ( $\lambda = 0.15406\text{ nm}$ ) operating at 30 kV and 16 mA to identify crystalline phases including the catalysts. X-Ray photoelectron spectra (XPS) were recorded using an ESCA3400 spectrometer (Shimadzu Co. Ltd) equipped with a Mg  $K_\alpha$  X-ray exciting source (1253.6 eV) operating at 10 kV and 20 mA. The binding energies (BE) referred to the C 1s peak at 285.0 eV.

## 2.3. Evaluation of catalytic activity for the hydrogenation of carbon dioxide into formic acid

The hydrogenation reaction of carbon dioxide was carried out in a 120 mL stainless steel autoclave with a magnetic stirrer (Taiatsu Techno). The catalyst was put into the autoclave with 5 mL of triethylamine and 17 mL of deionized water. The autoclave was heated to 393 K, and the reactor was then pressurized to 5 MPa with  $\text{H}_2$  followed by the introduction of carbon dioxide from a cooled (268 K) reservoir by a high-pressure liquid chromatography pump up to 13.0 MPa as a total pressure at which point the reaction was considered to have started and maintained for 1 h. After the reaction, ethyl acetate (2 mL) was added to the mixture as an internal standard for the quantitative analysis of the product, and the liquid mixture from the autoclave was analysed using a Shimadzu GC 8A gas chromatograph equipped with aa 15% TSG-1 on a SHINCARBON A column (Shimadzu,  $2\text{ m} \times 3\text{ mm}$ ) and a thermal conductivity detector. The yield was evaluated from the results in terms of the turnover number (TON) of formic acid, which is the number of moles of formic acid produced per mole of ruthenium.

## 3. Results and discussion

The influence of preparation conditions on the particle size of carbon sphere templates was investigated. Fig. 1 shows the particle size distribution of templates prepared with various glucose concentrations and settling temperatures before hydrothermal treatment to form template particles. From the distribution of samples prepared with various glucose concentrations (Fig. 1(a), (d) and (e)), it was observed that the size increased with the increase in glucose concentrations. However, the size first increased with the increase in settling temperature up to 348 K and then drastically decreased with the increase in temperature up to 373 K.

In order to identify the influence of the preparation conditions on the particle size of spherical carbon templates, the

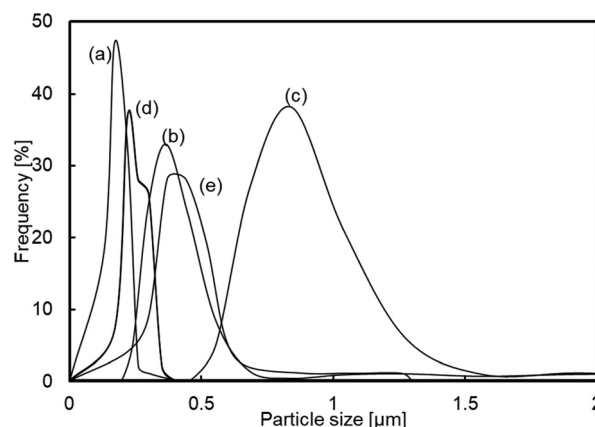


Fig. 1 The particle size distribution of spherical carbon templates prepared with (a) 16.05, (b)–(d) 21.40, and (e) 42.80 g of glucose. Settling temperatures: (b) 323, (c) 348, and (a), (d), and (e) 373 K.



starting glucose solution for the preparation of templates before and after settling the solution was analysed by FTIR-ATR spectroscopy, as shown in Fig. 2. All the spectra included bands assigned to exocyclic C–O stretching (*ca.* 993  $\text{cm}^{-1}$ ), C–H bending (*ca.* 1034  $\text{cm}^{-1}$ ), endocyclic C–O stretching (*ca.* 1079 and 1104  $\text{cm}^{-1}$ ), and  $\text{CH}_2$  wagging (*ca.* 1150  $\text{cm}^{-1}$ ) mode, respectively.<sup>32–34</sup> The band intensity at *ca.* 1079  $\text{cm}^{-1}$  in all the spectra of the solution after settling at various temperatures was high compared with the solution. The intensity increased with the order of settling temperatures of 348 K > 323 K > 373 K, while with the order of glucose concentrations of 42.80 g > 21.40 g > 16.05 g. From that and the result in Fig. 1, it is suggested that hydrolysis reaction of glucose at exocyclic hydroxyl groups proceeded with high degrees at high settling temperatures and in solutions with low glucose concentrations, resulting in a relatively high amount of endocyclic C–O bonds and templates with small size were obtaining following hydrothermal treatment. Fig. 3 displays the TEM images of hollow silica spheres prepared with the templates. Comparing the samples prepared with various glucose concentrations at 373 K (Fig. 3(a), (d), and (e)), the particle sizes of the hollow spheres prepared with 16.05, 21.40, and 42.80 g of glucose were *ca.* 170, 160 and 570 nm and the shell thickness were *ca.* 7, 14 and 85 nm, respectively. The shell thickness can also control with controlling the particle size of the templates because of increasing the amount of silica coated on the templates with decreasing the particle size of the templates. The result in Fig. 3(a), (d), and (e) can reflect the tendency of increasing the shell thickness with

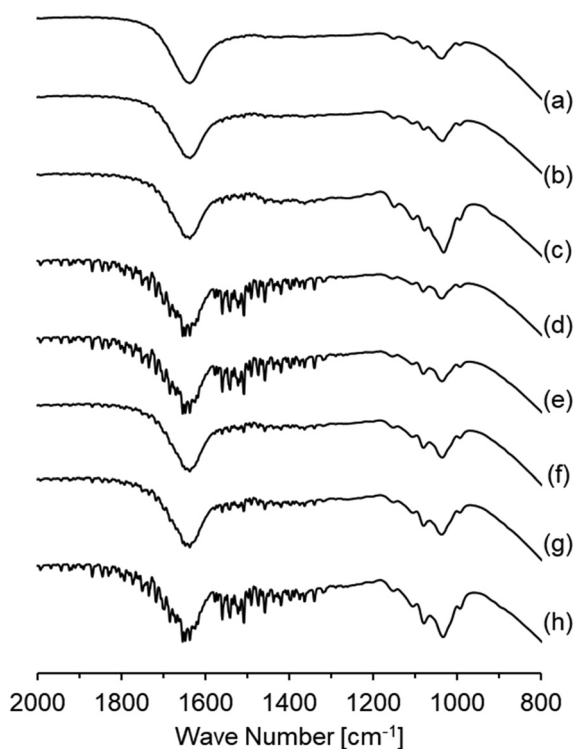


Fig. 2 FTIR-ATR spectra of aqueous solutions including (a), (d) 16.05, (b), (e)–(g) 21.40, and (c) and (h) 42.80 g of glucose before (a)–(c) and after settling at (e) 323, (f) 348, and (d), (g), (h) 373 K for 1 h.

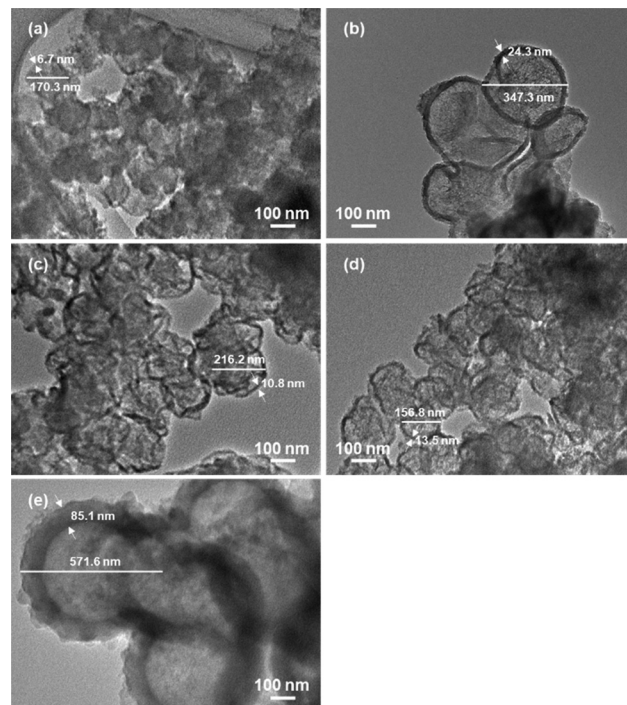


Fig. 3 TEM images of hollow silica spheres prepared with the glucose concentration of (a) 16.05, (b)–(d) 21.40, and (e) 42.80 g. Settling temperatures: (b) 323, (c) 348, and (a), (d), and (e) 373 K.

the increase in the particle size of templates. Otherwise, the particle size and shell thickness were not significantly affected by the settling temperatures. The result indicated that the particle size of hollow spheres, especially the hollow spheres prepared with templates with large particle size, decreased during calcination because of the shrinkage of particles accompanied by the decomposition of template particles.

With the hollow silica spheres, ruthenium-encapsulated hollow silica spheres were prepared and their activity for the hydrogenation of carbon dioxide was assessed. Table 1 lists the ratios of ruthenium to silicon and TON of the ruthenium-encapsulated catalysts. The Ru/Si ratios of the samples prepared with 21.40 g of glucose were influenced by settling temperatures before preparation of carbon sphere templates. The ratios tend to be high in the samples prepared with high settling temperatures. The highest TON to produce formic acid

Table 1 Compositions and activity of ruthenium-encapsulated hollow silica sphere catalysts prepared under various preparation conditions of carbon templates

Glucose (g)	Settling temp. (K)	Ru/Si <sup>a</sup> (–)	TON <sup>b</sup> (mol-HCOOH (mol-Ru) <sup>–1</sup> )
16.05	373	24.2	68.7
21.40	323	2.0	38.8
	348	26.4	29.6
	373	12.3	57.8
42.80	373	10.2	25.9

<sup>a</sup> Estimated from results of EDX analyses. <sup>b</sup> Estimated from results of GC-TCD analyses.





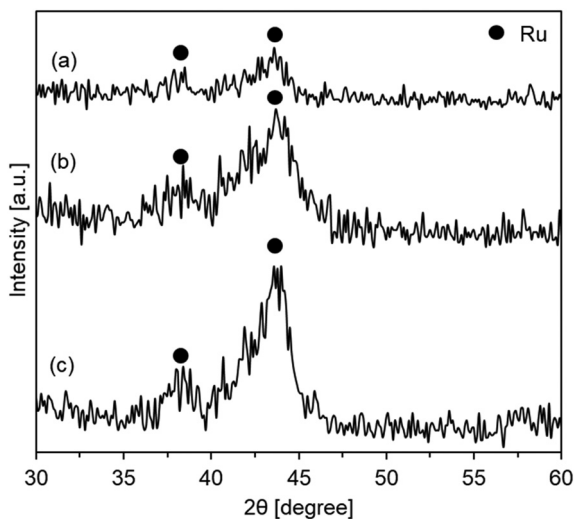


Fig. 4 Powder XRD profiles of ruthenium-encapsulated hollow silica sphere catalysts prepared with carbon sphere templates with (a) 16.05, (b) 21.40, and (c) 42.80 g of glucose after the catalytic hydrogenation of carbon dioxide.

was obtained in the presence of the catalyst prepared with 373 K settling temperature. The concentration of synthesized formic acid in the reaction solution was 11.7 vol% and the ratio of formic acid to triethyl amine was 2.16. The result indicated that the catalyst with appropriate amounts of highly dispersed active ruthenium species exhibited high activity for the hydrogenation of carbon dioxide into formic acid. However, the Ru/Si ratios decreased with the increase in glucose concentrations, indicating that the active ruthenium species were highly encapsulated in or supported on the hollow silica spheres with smaller diameters. The result reflected on their activity, and the catalyst including the smallest size of hollow spheres exhibited the highest TON. We have previously reported a ruthenium-supported silica catalyst for the hydrogenation of carbon dioxide into formic acid, and the activity of the catalyst in the present study was higher than that of the supported catalyst.<sup>35</sup> In addition, the catalyst activity was also comparative in comparison to the previous heterogeneous catalysts.<sup>12,15</sup>

In order to estimate the dispersion of the active ruthenium species, the XRD profiles of the catalysts prepared using templates prepared with various glucose concentrations after the catalytic hydrogenation of carbon dioxide were compared. As shown in Fig. 4, all the profiles included peaks at ca 38.0 and 43.5° assigned to the metallic Ru(100) and Ru(101) planes (JCPDS card no. 06-0663), respectively.<sup>36–39</sup> The peak intensity increased with the increase in glucose concentrations. The crystalline sizes of the active species were estimated using the Scherrer equation, and the crystalline sizes of the catalysts prepared with the templates using 16.05, 21.40, and 42.80 g of glucose were 3.6, 4.1, and 5.4 nm, respectively. The results indicated that the active metallic ruthenium species were highly dispersed on the hollow silica sphere support with a small diameter.

We also identified the dispersion of active species through morphological analysis of the catalyst after the catalytic

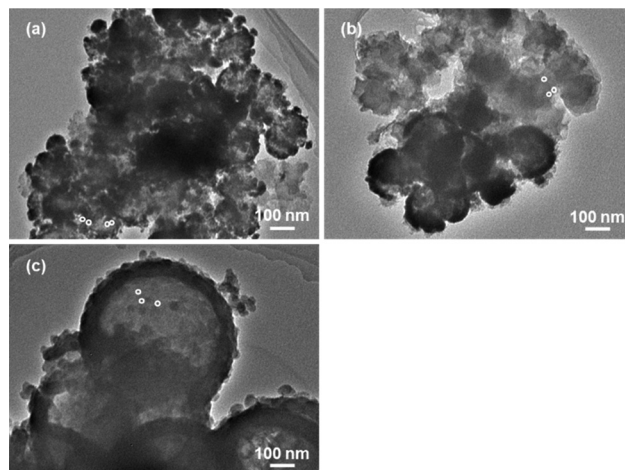


Fig. 5 TEM images of ruthenium-encapsulated hollow silica sphere catalysts prepared with templates prepared using (a) 16.05, (b) 21.40, and (c) 42.80 g of glucose after the catalytic hydrogenation of carbon dioxide.

hydrogenation of carbon dioxide, as shown in Fig. 5. From the images, all the catalysts included active ruthenium particles with a diameter of ca. 3–6 nm and larger secondary particles with a diameter of ca. 30–80 nm. The secondary particles could be agglomerates of small primary particles with a diameter of ca. 3–6 nm. However, the particle size growth of the active ruthenium species was not observed on the ruthenium-encapsulated hollow silica spheres, as reported in another work.<sup>40</sup> The results displayed in Fig. 4 and 5 indicated that the activity of the ruthenium-encapsulated hollow silica sphere catalyst was mainly influenced by the dispersion of primary particles of the active metallic ruthenium species, and the particle size of the active species did not significantly change before and after the catalytic reaction. Otherwise, the larger secondary particles may cause a relatively low activity in comparison to the previously reported catalysts.<sup>17</sup> The activity of the catalyst in the present study is expected to be improved by increasing the dispersion of the active species through the investigation of supporting methods of the active species on hollow silica spheres.

## 4. Conclusions

The present work investigated the influence of preparation conditions on the particle size and activity of ruthenium-encapsulated hollow silica sphere catalysts. The settling temperatures before hydrothermal treatment and the concentration of glucose solutions influenced the particle size of carbon sphere templates for preparing a hollow silica sphere support, and hollow spheres with small particle size were obtained at high settling temperatures and with low glucose concentrations. The result of FTIR-ATR spectroscopy of the glucose solution for preparing carbon sphere template particles indicated that the spectra of the solution at high settling temperatures and with low glucose concentration included the band assigned to the endocyclic C–O bond with a relatively



high intensity, indicating that hydrolysis reaction of glucose proceeded at high settling temperatures and in solutions with high glucose concentrations before hydrothermal treatment. The carbon sphere templates obtained following hydrothermal treatment included particles with small size. The result reflected the size of the hollow silica sphere support and the ruthenium-encapsulated catalysts. The catalysts with small particle size included highly dispersed active ruthenium species identified from the PXRD profiles and TEM images, and the catalyst exhibited high activity for the hydrogenation of carbon dioxide into formic acid.

## Author contributions

Syntheses, characterizations, and activity tests by E. Nagakubo, K. Saeki, and T. Umegaki; work led T. Umegaki and Y. Kojima; data analyses and manuscript writing by T. Umegaki; manuscript validation by all.

## Conflicts of interest

There are no conflicts to declare.

## References

- Q. Liu, L. Wu, R. Jackstell and M. Beller, *Nat. Commun.*, 2014, **6**, 5933.
- J. Artz, T. E. Müller and K. Thenert, *Chem. Rev.*, 2018, **118**, 434.
- M. D. Burkart, N. Hazari, C. L. Tway and E. L. Zeitler, *ACS Catal.*, 2019, **9**, 7937.
- R.-P. Ye, Y. Ding, W. Gong, M. D. Argyle, Q. Zhong, Y. Wang, C. K. Russell, Z. Xu, A. G. Russell, Q. Li, M. Fan and Y.-G. Yao, *Nat. Commun.*, 2019, **10**, 5698.
- S. Ezendam, M. Herran, L. Nan, C. Gruber, Y. Kang, F. Gröbmeyer, R. Lin, J. Gargiulo, A. Sousa-Castillo and E. Conrtes, *ACS Energy Lett.*, 2022, **7**, 778.
- M. Liu, Y. Xu, Y. Meng, L. Wang, H. Wang, Y. Huang, N. Onishi, L. Wang, Z. Fan and Y. Himeda, *Adv. Energy Mater.*, 2022, **12**, 2200817.
- M. S. Jeletic, M. T. Mock, A. M. Appel and J. C. Linehan, *J. Am. Chem. Soc.*, 2013, **135**, 11533.
- J. Su, L. Yang, M. Lu and H. Lin, *ChemSusChem*, 2015, **8**, 813.
- J. Su, M. Lu and H. Lin, *Green Chem.*, 2015, **17**, 2769.
- T. Umegaki, Y. Enomoto and Y. Kojima, *Catal. Sci. Technol.*, 2016, **6**, 409.
- W. H. Bernskoetter and N. Hazari, *Acc. Chem. Res.*, 2017, **50**, 1049.
- H. Zhong, M. Iguchi, M. Chatterjee, T. Ishizaka, M. Kitta, Q. Xu and H. Kawanami, *ACS Catal.*, 2018, **8**, 5355.
- K. Mori, T. Sano, H. Kobayashi and H. Yamashita, *J. Am. Chem. Soc.*, 2018, **140**, 8902.
- K. Nakajima, M. Tominaga, M. Waseda, H. Miura and T. Shishido, *ACS Sustainable Chem. Eng.*, 2019, **7**, 6522.
- Y. Kuwahara, Y. Fujie, T. Mihogi and H. Yamashita, *ACS Catal.*, 2020, **10**, 6356.
- D. Wei, R. Sang, P. Sponholz, H. Junge and M. Beller, *Nat. Energy*, 2022, **7**, 438.
- S. J. L. Anandaraj, L. Kang, S. DeBeer, A. Bordet and W. Leitner, *Small*, 2023, **19**, 2206806.
- Z. Zhang, F. Xiao, J. Xi, T. Sun, S. Xiao, H. Wang, S. Wang and Y. Liu, *Sci. Rep.*, 2014, **4**, 4053.
- H. A. Khan, P. Natarajan and K.-D. Jung, *Appl. Catal., B*, 2018, **231**, 151.
- X. Lin, S. Wang, W. Tu, H. Wang, Y. Hou, W. Dai and R. Xu, *ACS Appl. Energy Mater.*, 2019, **2**, 7670.
- T. Umegaki, H. Katori, K. Otake, R. Yamamoto and Y. Kojima, *J. Sol-Gel Sci. Technol.*, 2019, **92**, 715.
- T. Umegaki, K. Yabuuchi, N. Yoshida and Q. Xu, *New J. Chem.*, 2020, **44**, 450.
- C. Zhou, H. Ma, W. Yuan and F. Qi, *Catal. Commun.*, 2021, **149**, 106185.
- T. Umegaki, H. Ogawa, K. Watanabe, S. Ohki, M. Tansho, T. Shimizu and Y. Kojima, *Int. J. Hydrogen Energy*, 2021, **46**, 6659.
- K. Grzelak and M. Trejda, *Materials*, 2021, **14**, 7378.
- Z. Hu, M. Han, C. Chen, Z. Zou, Y. Shen, Z. Fu, X. Zhu, Y. Zhang, H. Zhang, H. Zhao and G. Wang, *Appl. Catal., B*, 2022, **306**, 121140.
- S. Ahn, K. Park, K. R. Lee, A. Haider, C. V. Nguyen, H. Jin, S. J. Yoo, S. Yoon and K.-D. Jung, *Chem. Eng. J.*, 2022, **442**, 136185.
- X. Sun and Y. Li, *Angew. Chem., Int. Ed.*, 2004, **43**, 597.
- X. Li, F. Chen, X. Lu, C. Ni, X. Zhao and Z. Chen, *J. Porous Mater.*, 2010, **17**, 297.
- L. Xu, L. Guo, G. Hu, J. Chen, X. Hu, S. Wang, W. Dai and M. Fan, *RSC Adv.*, 2015, **5**, 37964.
- Q. Wang, X. Y. Qian, L. N. Jin, X. Q. Shen, J. L. Tan and L. Wang, *J. Optoelect. Adv. Mater.*, 2020, **22**, 54.
- J.-J. Max and C. Chapados, *J. Phys. Chem. A*, 2007, **111**, 2679.
- J. Zakzeski, R. J. Grisel, A. T. Smit and B. M. Weckhuysen, *ChemSusChem*, 2021, **5**, 430.
- S. Roy, D. Perez-Guaita, D. W. Andrew, J. S. Richards, D. McNaughton, P. Heraud and B. R. Wood, *Anal. Chem.*, 2017, **89**, 5238.
- T. Umegaki, Y. Enomoto and Y. Kojima, *J. Jpn. Inst. Energy*, 2017, **96**, 332.
- R. V. Ranganathan, Z. Liu, H. Menon, S. Talukdar, R. Wang and M. Uddi, *Int. J. Energy Eng.*, 2020, **10**, 67.
- O. R. Fonseca-Cervantes, A. Pérez-Larios, V. H. R. Arellano, B. Sulbaran-Rangel and C. A. G. González, *Processes*, 2020, **8**, 1032.
- T. A. Hansu, O. Sahin, A. Caglar and H. Klvrak, *React. Kinet., Mech. Catal.*, 2020, **131**, 661.
- T. A. Hansu, *Int. J. Hydrogen Energy*, 2023, **48**, 6788.
- T. Umegaki, K. Saeki and Y. Kojima, *ACS Sus. Res. Manage.*, submitted.

